Bangladesh J. Bot. **52**(2): 437-443, 2023 (June) Special DOI: https://doi.org/10.3329/bjb.v52i20.68191

SOIL SALINITY, ITS INVERSION AND SPATIAL DISTRIBUTION CHARACTERISTICS IN AGRICULTURAL FIELDS USING REMOTE SENSING DATA

HUI KONG[1,2], DAN WU[2] AND LIANGYAN YANG[2]

Technology Innovation Center for Land Engineering and Human Settlements, Shaanxi Land Engineering Construction Group Co., Ltd and Xi'an Jiaotong University, Xi'an 710049, China

Keywords: Remote sensing, Farmland, NDWI, Soil salinity, Spatial distribution

Abstract

Soil salinization is an urgent problem in the arid and semi-arid regions that damages soil ecology and affects agricultural growths. Timely supervision and monitoring of soil salinity are essential to reach the most sustainable improvement goals in arid and semi-arid regions. In the present study, the soil of Aktau region in Xinjiang, China was collected to build a remote sensing based inversion model for identifying soil salinity hazards. Results showed that Normalized Difference Vegetation Index (NDVI), Normalized Difference Water Index (NDWI), and Difference Vegetation Index (DVI) were correlated ($P < 0.01$) with the model inversion, having correlation coefficients of -0.735, -0.858, and -0.774, respectively. All these were suitable for the construction of the soil salinity inversion model where the optimal parameters of model accuracy were above 85% and prediction results were accurate credible and consistent with the measured data. The NDWI extracted from multispectral images was used as the key parameter of the soil salinity inversion model, which could obtain a better spatial distribution of soil salinity. The remote sensing inversion model of soil salinity provides a theoretical basis for the management of soil salinization and sustainable utilization of agricultural resources in the Aktau region of Xinjiang.

Introduction

Soil salinization is a process in which salts from the bottom layer of soil or groundwater rise to the surface with capillary water (Yang and Wang 2015), and accumulate in the surface layer after evaporation (Zinck 2003). Due to the dry weather, high evaporation, and shallow depth of ground water in arid and semi-arid areas, a large amount of salts in the soil gather on the surface, causing salinization. The formation of soil salinization is being accelerated by irrigation, fertilization, and changes in depth of the water table. Salinization not only causes soil consolidation (Gorji *et al.* 2017), but affects crop growth, and leads to the abandonment and desertification (Zhang *et al.* 2018). For farmland, rapid monitoring of soil salinity can reveal the trend in salinity changes and adjust water management programs (Li and Wang 2015). Remote sensing can provide a rapid assessment of soil salinity. This information can be used to implement corrective treatments. The concept of rapid salinity monitoring will improve scientific understanding and sustainable utilization of saline fields. (Lobell and Asner 2002).

Zhou *et al.* (2019) used traditional vegetation index, enhanced vegetation index, and soil salinity index (Moussa *et al.* 2020) to establish inverse models with soil salinity for quantitative estimation and dynamic monitoring of the problem in the study area (Zhou *et al.* 2019). Using Landsat 8 OLI remote sensing images, indices of salinity, atmospheric impedance vegetation, soil regulating vegetation, and canopy response salinity were extracted to build inverse models (Feng *et al.* 2018). Along with soil salinity data, they have used three methods: multiple linear regression, partial least squares, and support vector machine (He *et al.* 2006).

*Author for correspondence: <2013127006@chd.edu.cn>.[1]Institute of Land Engineering and Technology, Shaanxi Land Engineering Construction Group Co., Ltd., Xi'an 710075, China. [2]Shaanxi Provincial Land Engineering Construction Group Co., Ltd, Xi'an 710075, China.

The present study was aimed to construct a soil salinity inversion model by using multispectral remote sensing satellite image data with vegetation index (NDVI), water body index (NDWI), and differential vegetation index (DVI) as the main inversion indices. To find optimal parameters for agricultural soils in Aketao County correlation calculations used (Tumaerbai *et al.* 2016). Furthermore, an improvement of the model was targeted by using the inversion methods of water body index and vegetation index, which were not considered in previous studies.

Materials and Methods

The study area was located in Aketao County, Xinjiang, situated in the western frontier of China, southwest of Xinjiang Uygur Autonomous Region. It is in the east of the Pamir Plateau, and the western edge of the Tarim Basin having geographical location between (732605~7643′ 31E, 374128~392955″ N) (Fig. 1), (Yang *et al.* 2014). The national border is more than 380 km long and covers an area of 24,176 km^2 (Tumaerbai *et al.* 2016). The climate of Aketao County is vertically distributed in three dimensions, and over a 10 km distance, the climate can range from frigid to thermic. It is a warm temperate continental arid climate, with drought and little rain and snow throughout the year, with an average annual temperature of 11.3°C and an average annual precipitation of 60 mm (Peng *et al.* 2016). The frost-free period is 221 days long, with a large temperature difference between day and night, and abundant light and heat resources, making it suitable for the growth of many kinds of crops and fruit trees (Wu *et al.* 2013). The plain farming areas are arid with lower precipitation, abundant sunlight, high evaporation, and with clearly distinct seasons (Allbed *et al.* 2014).

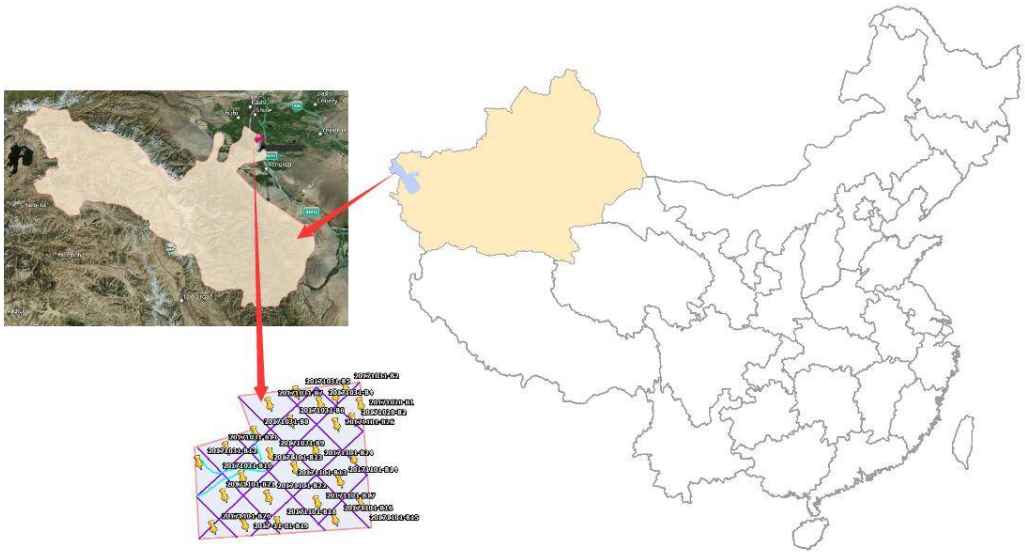

Fig. 1. Location diagram and sampling points.

The data source used for the present study was primarely Landsat series data. Beside Landsat image, PALSAR image should be included which suited to detect changes in topography and geology from signals reflected on the earth's surface, which are derived from the geospatial data cloud platform (http://www.gscloud.cn/). The data are pre-processed using ENVI5.3 and ArcGIS10.8 platforms for, including geometric, and radiation corrections, Flash atmospheric corrections, and color synthesis, etc. Six types of indices related to soil salinity were selected

(Douaoui 2017), namely brightness index (BI), salinity indices (normalized difference salinity index NDSI, salinity index SI), vegetation index NDVI, water body index NDWI and differential vegetation index DVI (Table 1). In the present study water body index and other remote sensing indices were used to construct the soil salinity inversion model, combined with the local land-use classification status to exclude the influencing factors, only the salinization status of the farmland area was studied.

Table 1. Spectral index calculation formula.

Spectral index	Calculation formula
BI	$\sqrt{r^2 + NIR^2}$
NDSI	$(r - NIR) / (r + NIR)$
SI	$\sqrt{b * r}$
NDVI	$(NIR - r) / (NIR + r)$
NDWI	$(g - NIR) / (g + NIR)$
DVI	$NIR - r$

r is the red band, g is the green band, b is the blue band, and NIR is the near infrared band in the table.

The sampling points of the fields were visited prior to investigation of the surface characteristics, salinization status, uniformity, and representativeness of the sampling points in the study area, and sample points were collected using a global positioning system (GPS). Afterwards, the soil samples were processed for indoor testing; a total of 70 soil samples were obtained, 10 invalid sampling points were removed, and 60 valid sampling points were left. Thirty four points were used to build the model and 26 points were used for validation. sixty soil samples were dried and ground naturally, and their electrical conductivity was measured after passing through a soil screen with a diameter of 2 mm. Their conductivity values were measured, and the soil salt content (SSC, g/kg) was calculated by the empirical formula, which is SSC = (0.2882EC5:1 + 0.0183) (Yao *et al.* 2013). According to the national soil salinity grading standard, the soil was classified into five levels, with soil containing < 1 g/kg of salt as non-saline soil, 1-3 g/kg as lightly saline soil, 3-6 g/kg as moderately saline soil, 6-15 g/kg as heavily saline soil, and >15 g/kg as saline soil (Zhang *et al.* 2011).

According to the sampled points, the sample points for validation were selected, and the constructed soil salinity inversion model was used to test, and the stability of the model and the evaluation index of prediction accuracy were judged by the coefficient of determination R2 and root mean square error RMSE, and the test expressions were.

$$R^2 = \frac{\sum_{i=1}^{n}(X_i=X)*(Y_i-Y)}{\sqrt{\sum_{i=1}^{n}(X_i=X)^2*\sum_{i=1}^{n}(Y_i=Y)^2}} \quad (1)$$

Where, n is the number of sampling points; X is the average of the measured values of soil sample i; Y is the predicted value of soil sample i; Y is the actual measured value; X is the average of the predicted values of soil sample actual for soil sample.

$$RMSE = \sqrt{\frac{\sum_{i=1}^{n}(Y_i^0 - Y_i^S)^2}{n}} \quad (2)$$

Where, n is the number of sampling points; Y and Ys are the predicted and simulated values of soil sample i, respectively.

Results and Discussion

The correlation between the multispectral indices and soil salinity showed that NDWI, NDSI, NDVI, DVI, BI, and SI were highly and significantly correlated with soil salinity content ($P < 0.01$) (Table 2). The correlation coefficients of NDVI and NDSI and were -1, respectively, indicating no difference. Therefore, three representative spectral indices with high correlation coefficients with soil salinity content were selected for this study: NDVI, NDWI and DVI.

Table 2. Correlation between soil salinity and spectral index.

	SSC	BI	NDSI	SI	NDVI	NDWI	DVI
SSC	1						
BI	-0.517**	1					
NDSI	0.793**	-0.441**	1				
SI	0.452**	0.296**	0.686**	1			
NDVI	-0.735**	0.431**	-1.000**	-0.679**	1		
NDWI	0.858**	-0.562**	0.932**	0.625**	-0.963**	1	
DVI	-0.747**	0.768**	-0.928**	-0.356**	-0.917**	-0.927**	1

**represents highly significant correlation ($P < 0.01$).

Results of the linear and quadratic fitting of the measured soil salinity data with each spectral parameter showed the significant and highly significant correlations between the soil salinity and each spectral index (Table 3). The linear and quadratic models were significantly correlated with each other and the accuracy of the models were around 85%, so NDWI,NDVI and DVI can be used for model construction and the accuracy of the models is high.

Table 3. Models for estimating soil salinity with different spectral indices.

Spectral index	Model type	Estimation model	R	R^2	P
NDVI	Linear	$Y=16.648-31.187x$	0.846	0.716	0.005**
NDVI	Quadratic	$Y=23.982-75.846x+57.742x^2$	0.853	0.728	0.001**
NDWI	Linear	$Y=20.39-34.76x$	0.881	0.776	0.001**
NDWI	Quadratic	$Y=29.783-83.351x+55.471x^2$	0.895	0.801	0.007**
DVI	Linear	$Y=13.932-52.869x$	0.817	0.667	0.017**
DVI	Quadratic	$Y=21.392-145.67x+226.12x^2$	0.833	0.694	0.024**

Y represents soil salinity content; x represents spectral parameters; **indicates highly significant correlation ($p < 0.01$).

The linear-model and quadratic-model constructed by soil salinity and NDVI, NDWI and DVI can effectively reflect the soil salinization condition. Based on the further improvement with the accuracy of the models, this study combined soil salinity and three indexes measured salinity values that had a coefficient of determination i.e. 0.817. remote sensing images to establish a quadratic model.

The model was as follows:

$$SSC = 66.925 * NDWI^2 - 55.066 * NDVI^2 + 154.046 * DVI^2 + 101.339 * NDWI + 53.81 * NDVI - 62.508 * DVI + 29.492$$

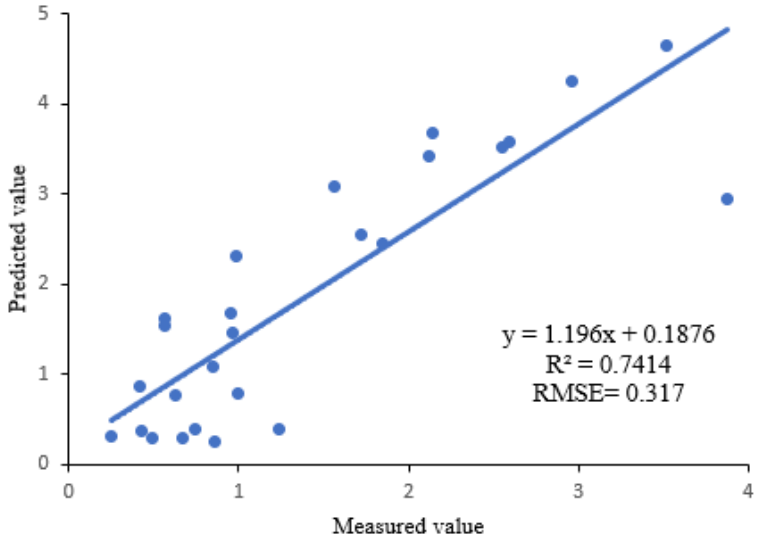

Fig. 2. Data validation fit plots.

The validation of the model is shown in Fig 2. It can be seen from that the measured and predicted values were highly corrected to each other (r^2= 0.74). The model root mean square error is of 0.317.

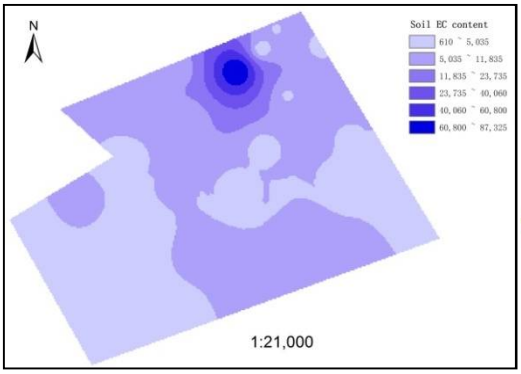

Fig. 3. Spatial distribution of soil conductivity.

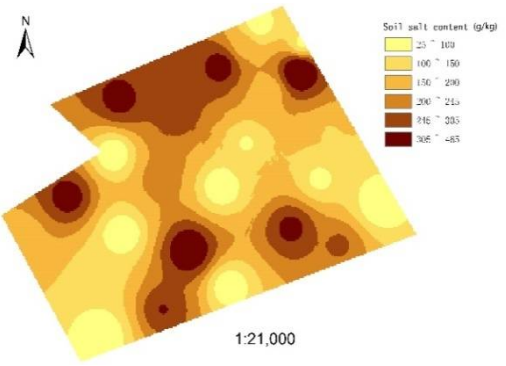

Fig. 4. Spatial distribution of soil salinity.

The spatial distribution of soil salinity in the study area was inferred according to the best soil salinity inversion model (Figs 3-4). From the overall viewpoint of which Shihezi irrigation area has the most serious soil salinity, followed by Jinguhe irrigation area, and Mosowan irrigation area has the least soil salinity.

In the present study, the soil of farmland in Aketao County was used as the research object, and the most suitable soil salinity inversion model was explored by constructing a soil salinity

inversion model to predict the soil salinity in the study area using a combination of measured data and multispectral remote sensing image data, and the conclusions are as follows:

(1) Based on the correlation analysis between the spectral indices and soil salinity, three representative spectral indices with high correlation with soil salinity were selected: NDVI, NDWI and DVI. The correlation coefficients were -0.735, -0858 and -0.774, respectively. The inverse models were constructed with soil salinity, and the modeling accuracy was above 85%, reaching a highly significant level, and all of them could be used for (2). The inverse model of soil salinity was constructed in this study.

(2) The validation accuracy of the inverse model of soil salinity in this study reached 0.740, which is highly significant, and can predict the spatial distribution and distribution characteristics of soil salinity in oasis farmland in Aketao County more accurately.

(3) The soil salinity content of Aketao County is dominated by moderate and heavy saline soils, among which the salinity of Shihezi irrigation area is the most serious and that of Mosowan irrigation area is less saline. The predicted soil salinity content in the study area is more consistent with the soil salinity content in the actual sampling sites. The study has important practical significance for the rapid extraction of salinization status and its prevention and control in Aketao County.

Acknowledgements

Supported by Funded by Technology Innovation Center for Land Engineering and Human Settlements, Shaanxi Land Engineering Construction Group Co.,Ltd and Xi'an Jiaotong University(2021WHZ0088) and Soil moisture inversion study of the Loess Plateau dry plateau based on SAR radar data(DJNY2022-23).and Key Research and Development Program of Shaanxi under Grant 2022ZDLNY02-10.

References

Allbed A, Kumar A and Aldakheel Yousef Y 2014. Assessing soil salinity using soil salinity and vegetation indices derived from IKONOS high-spatial resolution imageries: Applications in a date palm dominated region. Geoderma **230-231**(7): 1-8.

Douaoui A, Nicolas H and Walter C 2017. Detecting salinity hazards within a semiarid context by means of combining soil and remote-sensing data. Geoderma **134**(1-2), 217-230.

Feng J, Ding J, Yang A and Cai L 2018. Remote sensing modeling of soil salinization information in arid areas. Agricul. Res. Arid Areas **36**(1): 266-273.

Hu D,·Tumaerbai Zhao Y *et al.* 2016. Study on characteristics of cotton field soil salt accumulation under perennial mulched drip irrigation in northern Xinjiang. J. Irriga. and Drain. **35**(1): 1-5.

He T, Wang J, Cheng Y *et al.* 2006. Spectral Features of Soil Moisture. Acta Pedologica Sinica **43**(6): 1027-1027.

Li B and Wang Y 2015. Radar inversion and simulation of salty soil salinization. J. Arid Land Resou. Environ. **29**(8): 180-184.

Lobell DB and Asner GP 2002. Moisture Effects on Soil Reflectance. Soil Sci. Soc. Amer. J. **66**(3): 722-727.

Moussa I, Walter C, Michot D *et al.* 2020. Remote sensing soil salinity assessment in irrigated paddy fields of the niger valley using a four-year time series of sentinel-2 satellite images. Remote Sensing **12**(20): 3399.

Peng L, Wang L, Liu H *et al.* 2016. Effects of irrigation conditions on the soil salinization distribution in the Oasis of arid area. Res. Soil Water Conserv. **23**(03): 112-118+124.

Taha Gorji, Elif Sertel and Aysegul Tanik. 2017. Monitoring soil salinity via remote sensing technology under data scarce conditions: a case study from Turkey. Ecol. Indicat. **74**: 384-391

Wu Y, Liu G and Yang J *et al.* 2013. Interpreting method of regional soil salinity 3D distribution based on inverse distance weighting. Transa. Chinese Soc. Agricul. Engin. **29**(3): 100-106.

Yang H, Zhang F and Wang D *et al*. 2014. The analysis of the variation trend and influencing factors of evapotranspiration in oasis along Manas river valley in the last 60 years. J. Arid Land Resou. Environ. **28**(7):18-23.

Yang Z and Wang B 2015. Present Status of Saline Soil Resources and Countermeasures for Improvement and Utilization in China. Shandong Agricul. Sci. **47**(4):125-130.

Yao Y, Ding J, Zhang F *et al*. 2013. Research on Model of Soil Salinization Monitoring Based on Hyperspectral Index and EM38. Spectros. Spect. Anal. **33**(6): 1658-1664.

Zhang TT, Zeng SL, Yu G *et al.*2011. Using hyperspectral vegetation indices as a proxy to monitor soil salinity. Ecol. Indicators **11**(6): 1552-1562.

Zhang XL, Zhang F, Zhang HW *et al*. 2018 Optimization of a hyperspectral index soil salinity inversion model based on spectral transformation. J. Agri. Engin. **34**(1):110-117.

Zhou X, Zhang F, Zhang H *et al*. 2019. A Study of Soil Salinity Inversion Based on Multispectral Remote Sensing Index in Ebinur Lake Wetland Nature Reserve. Spectros. Spect. Anal. **39**(004): 1229-1235.

Zinck G 2003. Remote sensing of soil salinity: potentials and constraints. Remote Sens. Environ. **85**(1): 1-20.

(Manuscript received on 18 March, 2022; revised on 07 August, 2022)